ANALYSIS AND DESIGN OF ANGLE CONTROLLED CURRENT SOURCE INVERTER FED INDUCTION MOTOR DRIVE +

Mohammad Hussein baker *

Abstract:

The current source inverter-fed induction motor drive (hereafter referred to as CSIM drive) is one of widely used drives in the industry. Of the many strategies employed for the control of CSIM drive, angle control is the simplest scheme incorporate the aspect of "frequency compensation", thus paving the way for a fast response CSIM drive.

A step by step design of the angle-controlled CSIM drive is described.A systematic design of inner current loop, slip speed loop, outer speed loop, and frequency compensation loop is given. The design incorporates a linear relationship between the reference input and output of electromagnetic torque and strategy to obtain maximum torque per ampere. The commutation delay in the current source inverter is taken care of in the design of the frequency compensator.

Experimental results are given in support of the design procedure.

المستخلص:

مصدر التيار العاكس يجهز تغذية محرك حثي (يرمز له CSIM مجهز) والنظام المنسق هو واحد من الأستخدامات التي تستعمل على نطاق واسع في الصناعة. العديد من الاستراتيجيات المستخدمة (CSIM) بتجهيز زاوية السيطرة على ابسط خطة لإدماج الجانب من (التردد التعويضي) مما يمهد الطريق بسرعة استجابة (CSIM) المجهز.

خطوة فخطوة تصمم الزاوية التي يسيطر عليها (CSIM) المجهز يمكن وصفها من خلال الخطوات التالية:(١-منهجية التصميم من داخل حلقة التيار. ٢-حلقة السرعة المنزلقة .٣-حلقة سرعة المستخدم .٤-حلقة التردد التعويضي المعطاة).

التصميم يتظمن العلاقة الخطية بين اشارة الأدخال واشارة الأخراج للعزم الكهرومغناطيسي،ان ستراتيجية الحصول على اقصى عزم لكل امبير لتأخير التوحيد للتيار في مصدر العاكس يأخذ التصميم للتردد المعوض بنظر الأعتبار.

نتائج التجارب تعطي دعماً للتصميم الأجرائي.

Introduction:

The current source inverter-fed induction motor (CSIM) drive has been for a 1972 we are in 2007 [1] for the reason that it provides a precise and fast control of electromagnetic torque and a rugged four-quadrant operation with a minimum number of switching elements in its power circuit. The CSIM drive considered here consists

---

+ **Received on 5/11/2007 , Accepted on 22/12/2008**
* **Asst. Lecturer / Technical Instructors Training Institute**

of a front-end current source, a dc link filter an miosequential commutated current inverter, and an induction motor as shown in fig. 1.[1]

The front-end current source is obtained using a three-phase fully controlled bridge rectifier fed from a three-phase ac supply.

Three predominant schemes emerged for the control of CSIM drive:

1) field oriented control [2],
2) synchronous control [3],[4],
3) angle control [5]'

Sufficient literature is available for the design of CSIM drives with field-oriented and synchronous control strategies. For the angle-controlled CSIM drive, the situation is altogether different in that there are only two sources for its design [5], [6]. They cover only the control philosophy rather than that of the design details.

All three fast response strategies have a common denominator in that they have instantaneous torque angle correction along with the magnitude control of stator current for load torque disturbance and reference frequency change. This aspect is identified and is known as "frequency compensation" [6], [7]. The angle control scheme is the only scheme to incorporate the frequency compensation in the simplest manner. There in lies the ingenuity of the scheme the distinguishing aspect of the angle-controlled CSIM drive its angle loop or frequency compensation loop. The design of the inner current loop, outer speed loop, slip speed loop, frequency compensation loop, and the speed controller constitutes the core of the angle-controlled CSIM drive. For better utilization of the drive, the maximum torque per ampere is to be implemented. The design strategy to obtain a linear relationship between a torque reference and output of electromagnetic torque is given. The frequency compensator design is made after taking into account the effect due to current source inverter commutation delay.

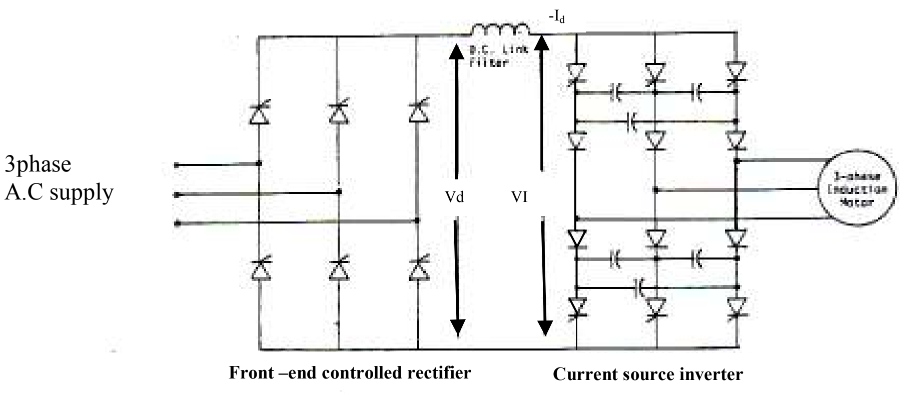

Fig.(1): Current Source induction motor drives

Angle-Controlled CSIM Drive:

The block diagram of the angle-controlled CSIM drive is shown in fig.2. The inner current loop consists of a controlled rectifier and the dc link H_1 and G_3. The unity gain speed loop is made up of G_{12}, G_{11}, G_{10}, G_7, G_D the inverter, and induction motor. The slip speed input is y_2, and the necessary angle adjustment for reference speed change and load torque disturbance is y_3. G_1 is the speed controller and G_2 is the current reference controller. The transfer functions of the controllers are all listed in Appendix 1.

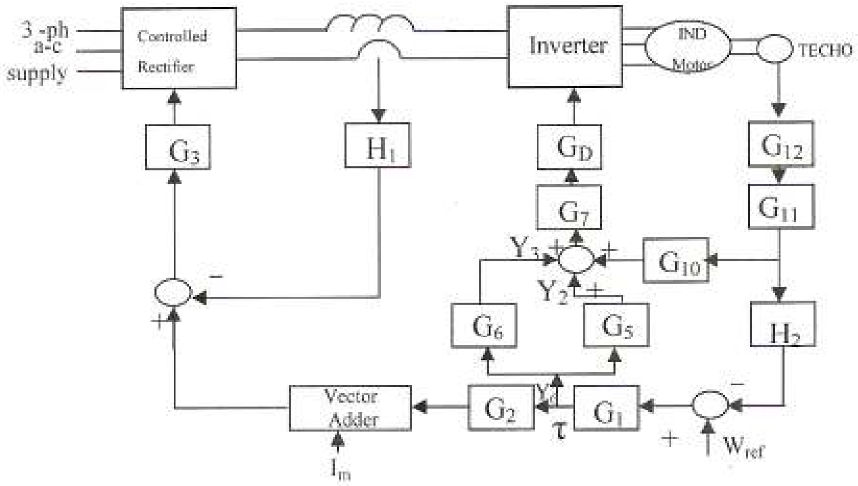

Fig.(2): block diagram of angle controlled CSIM drive.[7]

<u>Design of Current Control Loo:</u>

Synthesis of the current loop is difficult because:

1) The input impedance of the induction motor varies with load condition.
2) The operating point is dependent upon many factors such as load torque, stator frequency, and machine saturation.

The operating equations, even for a small-signal disturbance, will become four, and hence a straightforward approach is ruled on. A simple and direct design of the current loop is possible by considering the physical insight provided by the steady state equivalent circuit. The following assumptions are made:

1- Air gap flux is constant.
2- Change in load condition is reflected in the equivalent rotor resistance.
3- Stator is wye-connected.

Then the load and dc link with the current loop is of the form given in fig.3. The dc link filter and the stator can be represented by a block diagram, and its transfer function is given by:[7]

$$G_I(s) = \frac{1}{(R+2L)} \qquad (1)$$

where:

$$R = R_F + 2R_s \qquad (2)$$

$$L = L_F + 2L_{ls} \qquad (3)$$

$G_1(s)$ is an impedance function.

The delay in converter firing is represented by a transfer function of first-order pade approximation given as:

$$G_{de}(s) = \frac{1-bs}{1+bs} \qquad (4)$$

where:

1. 2b=I= statistical average of delay= 1/12 of ac input waveform = (1/12)×(1/60) S.[7] (5)

2. The first order approximation is valid for frequency up to 570 rad/s with negligible error up to 750 rad/s. Also, the functional e^{-Ts} is replaced by the rational transfer function suited to linear design techniques. The overall block diagram of the current loop is given in fig.4.

I

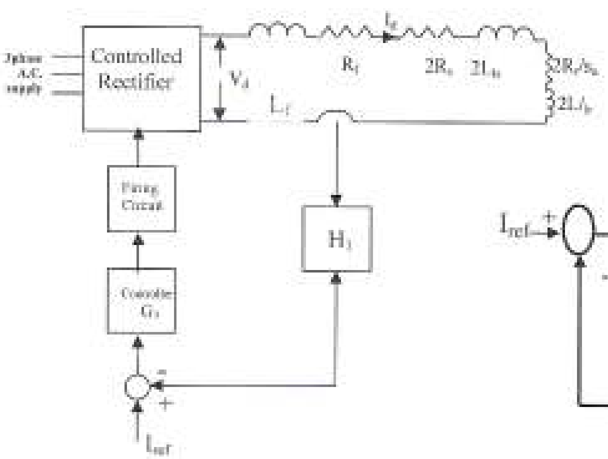

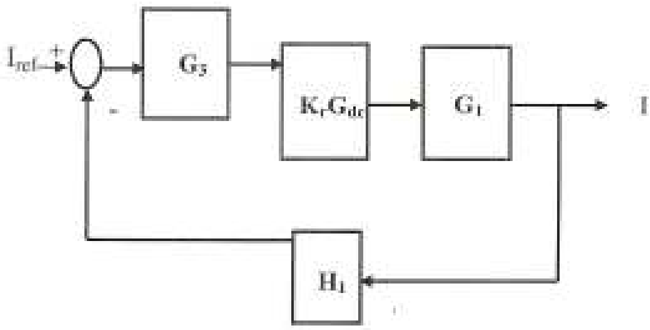

Fig. (3): Current control loop with load **Fig. (4):** overall diagram of current control loop

<u>Design of Current Controller:</u>

The current controller is chosen to be a proportional and integral controller of the form:

$$G_c(s) = k_3 \frac{(1+sTc)}{s} \qquad (6)$$

The transfer function of the link current and its reference is:

$$\frac{I_d}{I_{ref}}(S) = \frac{\frac{k_c(1+sTc)}{s}.k_R G_{dc} - \frac{1}{R(1+s\frac{L}{R})}}{1 + H_1 k_c \frac{(1+sTc)}{s}.k_R G_{dc} \frac{1}{R(1+\frac{L}{R})}} \qquad (7)$$

Let:

$$T_c = \frac{L}{R} \qquad (8)$$

Substituting (8) in (7):

$$\frac{I_d}{I_{ref}}(S) = \frac{\frac{k_c k_R G_{dc}}{R}}{s + \frac{H_1 k_c k_R G_{dc}}{R}} \tag{9}$$

$$\frac{I_d}{I_{ref}}(S) = \frac{k_a}{s + k_b} \tag{10}$$

where:

$$k_a = \frac{k_c k_R G_{dc}}{R} \tag{11}$$

$$k_b = H_1 k_a \tag{12}$$

Depending on the value of the gain of the current controller k_c, the rise time of the link current is controlled. The delay time in the converter can be overcome by adding a derivative of the current error signal to the control signal. The controller given in (6) is realized as shown in fig.5. The Zener clamps are to limit the control signal on the lower and higher levels. For safe operation during inversion, The maximum triggering angle of the controlled rectifier is limited to 155^o. A linear relationship between the control signal and the output link voltage in the converter is obtained with cosine inverse firing of the converter.

Fig

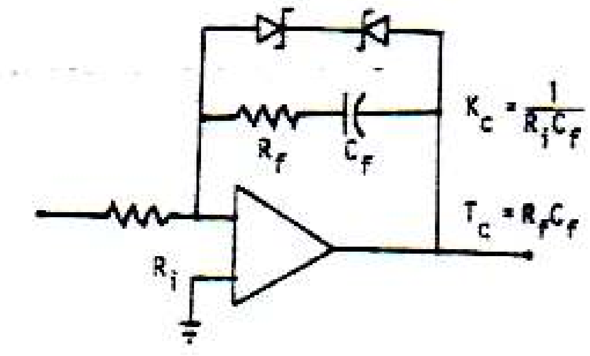

Fig. (5): Current controller realization

I. Strategy for Maximum Torque per Ampere and the Design of Current Reference Controller:

The optimum utilization of the drive, maximum torque per ampere must be extracted from the drive. The implementation criterion for such a strategy is developed from the steady-state operating of the induction motor. The electromagnetic torque of the induction motor is:[8]

$$T_e = \frac{\sum T}{R_r} \cdot \frac{W_{st}}{1+(W_{st}T_r)^2} \cdot [I_r^2 + I_m^2] \qquad (13)$$

where:

$$T_r = \frac{(I_m + L_{tr})}{R_r} \qquad (14)$$

$$W_{st}=3W_e \qquad (15)$$

I_m and I_r are the flux and torque producing components of the stator current, respectively. All other symbols are defined in the Nomenclature at the end of the paper.For maximum torque per ampere, the criterion is:

$$I_m=I_r \qquad (16)$$

In this case, the drive has a variable air gap flux for varying load conditions. From a practical point of view, to have the motor operating with a certain minimum level of flux is desirable even under no load condition. This is to enable the fast generation of electromagnetic torque up to the value corresponding to the minimum level flux. Therefore, the minimum level of the flux up to some load is chosen on the basis of load and dynamic requirements of the drive for the present. This will be fixed at 0.25 pu.

Hence the magnetizating current versus rotor current relationship is slightly modified from (16) and is shown in fig.6. From this figure, the stator current reference is obtained as:

$$\left.\begin{aligned} I_{s,ref} &= \sqrt{(0.25)^2 + (I_r)^2}\ , && 0 < I_r < 0.25 \text{ pu} \\ I_{s,ref} &= \sqrt{2}\, I_r\ , && 0.25 \le I_r \le 1.00 \\ I_{s,ref} &= \sqrt{1+(I_r)^2}\ , && I_r > 1.00 \text{ pu} \end{aligned}\right\} \qquad (17)$$

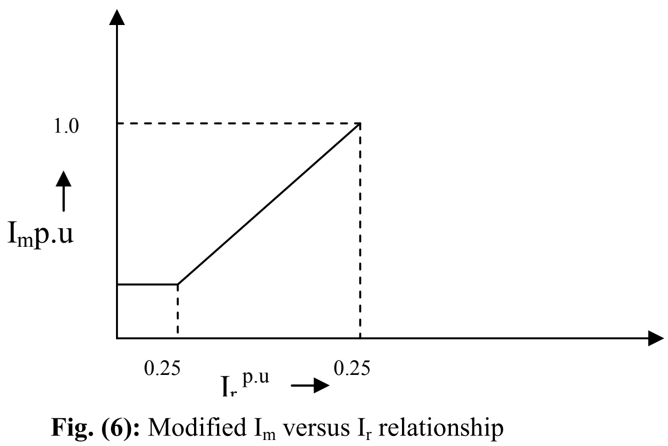

Fig. (6): Modified I_m versus I_r relationship

II. Design of Linear Relationship Between Reference Input and Output of Electromagnetic Torque:

Linearity in the input-output relationship of electromagnetic torque is necessity for torque regulated drives. This relationship is enforced by coordinating the stator current reference and slip frequency considering the outer speed loop and slip frequency loop of the angle control scheme show in fig.7; the blocks to be interrelated are G_2 and G_5.

Writing the outputs W_{st}, I_r as functions of the torque reference:

$$W_{st}=k_5T \tag{18}$$

$$I_r=k_2T=I_m \tag{19}$$

Substituting (18) and (19) in (13):

$$T_e=\frac{k_t}{R_r}\frac{k_5T}{1+(k_5\tau T_r)^2}2k_2^2\tau^2 \tag{20}$$

For T_e versus τ linearity, let:

$$1+(k_5\tau T_r)^2=k_5k_2^2\tau^2 \tag{21}$$

i.e. $k_5^2[T_r^2\tau^2]-k_5[k_2^2\tau^2]+1=0$ (22)

$$k_5=\frac{k_2^2\tau^2\pm\sqrt{k_2^2\tau^2-4T_r^2\tau^2}}{2\tau^2T_r^2} \tag{23}$$

$$W_{st}=k_5\tau=[\frac{k_2^2}{2T_r^2}]\tau\pm\sqrt{[\frac{k_2^2}{2T_r^2}]\tau^2-\frac{1}{T_r^2}} \tag{24}$$

The flow chart for the computation of slip frequency W_{st} is given in fig.8. Note that this could be implemented with available analog components.

Substituting the value of (22) in (20):

$$T_e=[\frac{2kt}{R_r}]\tau \tag{25}$$

using (19) in (25):

$$T_{e\max}=\frac{2k_r}{R_r}\frac{I_r}{k_2}=\frac{2k_r}{R_r}\frac{I_m}{k_2} \tag{26}$$

$$=k_{ta}I_r=k_{ta}I_m \tag{27}$$

where:

$$k_{ta}=\frac{2k_t}{k_2R_r} \tag{28}$$

Equation (27) corresponds to a dc motor drive with either a constant field excitation or with constant armature current.

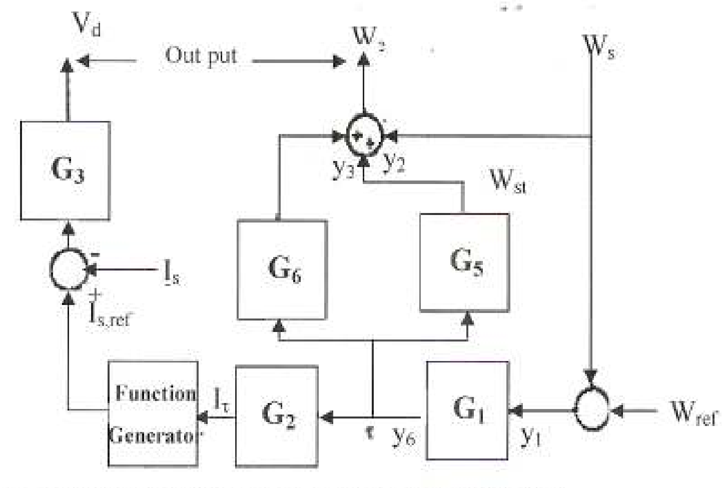

Fig. (7): Outer speed loop and slip speed loop of CSIM drive

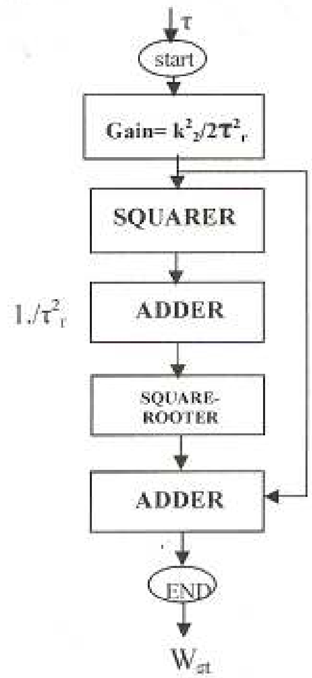

Fig. (8): Flow chart of computation of slip frequency

III. Design of Frequency Compensator and the Speed Controller:

The frequency compensator supplies the incremental stator frequency to move the stator current phasor in phase, during load torque disturbance and frequency reference changes. The design of this block then needs an understanding of the commutation delay. A numerical quantification of commutation delay for an operating point from the simple steady-state equivalent of the induction motor and its incorporation in the design via a second-order pade approximation of e^{-Td^s} is accomplished.

- **Commutation Delay in the Inverter**

Hitherto, the inverter output frequency is assumed to follow the frequency input command without a time delay. In an actual motor drive system a delay dependent on the motor operating point exists [6].

Around a steady-state operating point, the commutation time is calculated either numerically, solving the system transcendental equations of the CSIM drive [7], [8] or using the simplified expression given in [9]. The maximum error involved in using the simplified expression is less than two percent in comparison with the rigorous solution. This expression for commutation delay time is given in (29) and is used in this study.[8] , [9]

$$T_d = 5.73 W_e L_{ts} C + \sqrt{3 L_t C}.(1 + \pi / 2) \quad (29)$$

Where:

$$L_b = \frac{(\frac{R_r}{W_{st}})^2 (L_m - L_{tr}) - L_{tr}^2 (L_m + L_{tr})}{(\frac{R_r}{W_{st}})^2 + (L_m + L_{tr})^2} \quad (30)$$

- **Design of frequency compensator:**

The frequency compensator supplies an incremental frequency at the time of load torque disturbance and reference frequency change. Its output is proportional to the rate of change of torque angle. In the angle-controlled scheme, the torque angle is not measured. Therefore, the torque angle change is to be reconstructed from other available measurements. One such variable normally available is the torque reference signal generated through the slip speed. The torque angle change can be written in terms of other variables:

$$\frac{d\theta}{dt} = (\frac{d\theta}{ds_s}).(\frac{ds_s}{dt}) \quad (31)$$

The relationship between the torque angle and slip speed is fixed regardless of the magnitude of current for a particular value of motor resistance. The value of the rotor resistance used is that of the average operating temperature. Writing:

$$\frac{d\theta}{dt} = k(S_s).\frac{dS_s}{dt} \quad (32)$$

Where:

$$k(S_s) = \frac{d\theta}{dS_s} \quad (33)$$

$k(S_s)$ versus S_s can be programmed in the form of function generator or in the read only memory of the digital circuit. For the drive given in Appendix II, the value of the $k(S_s)$ varies by 60 times with in zero to full-load torque region, as seen from table 1. To compute (32), the rest that is needed is to compute the time derivative of the slip speed. The realization of the rate of change of torque angle is given in fig.9.

The gain k_a in the time derivative loop is used to offset the effect of inverter commutation delay T_d. Keeping:

$$k_a \propto T_d \tag{34}$$

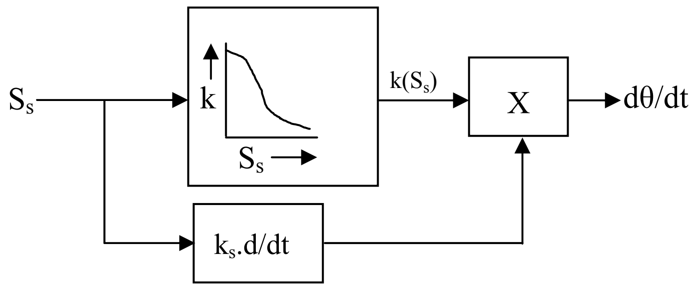

Fig. (9): Realization of rate of change of torque angle

Table (1): Slip Speed Versus $k(S_s)$

Slip Speed, rpm	$K(S_s)$
10	15.71
30	9.01
50	4.76
70	2.71
90	1.67
110	1.08
130	0.72
150	0.49
170	0.33
190	0.22

Gives a flexibility to assign the desired level of compensation delay T_d from (29) is seen to be the sum of a constant term and a variable term. The variable term is proportional to the product of load dependent L_b and the stator frequency W_e. The realization of T_d is shown in fig.10. L_b versus S_s can be programmed in a read only memory or obtained through a function generator. The relevant information is shown in table II. Then the final step is to incorporate the computed gain k_a into fig.9, to evaluate the rate of change of torque angle, It I given in fig.11. Both $k(S_s)$ and L_b are dependent upon the rotor resistance, which is quite sensitive to temperature variation. To account for rotor resistance sensitivity, a parameter adaption scheme [10] may be used to estimate the rotor time constant. Then the estimated value can be employed to modify both $k(S_s)$ and L_b.

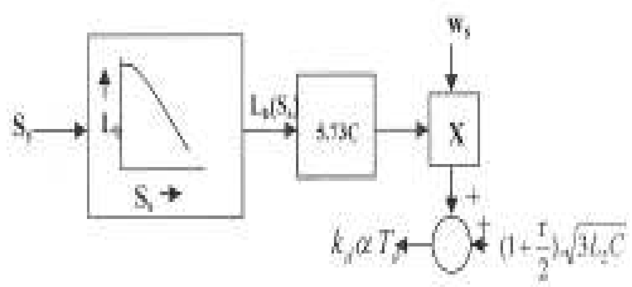

Fig. (10): Realization of time delay

Table (2): Slip Speed Versus L_b

Slip Speed, rpm	**L_b, Henry**
10	0.5701
30	0.3288
50	0.1778
70	0.1503
90	0.0681
110	0.0473
130	0.0346
150	0.0263
170	0.0206
190	0.0166

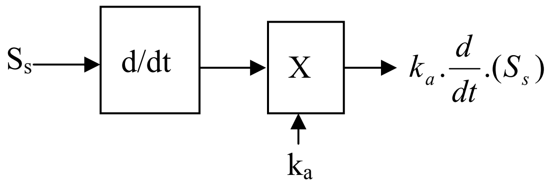

Fig. (11): Incorporation of k_a in slip speed derivative loop

- **Design of Speed Controller:**

With the design of the current controller current reference controller, slip speed controller, and frequency compensator completed, the remaining things to be considered are the design of the speed controller and the unity speed feedback loop. In the unity speed loop, the filter is carefully chosen with a view to minimize the time delay as well as to keep the ripple in the tachogenerator feedback to an acceptable level.The speed controller G_1 is designed by obtaining the open loop transfer function between y_1 and y_6, and using the Bode plot, the values of the controller gain and time constants are evaluated. This approach takes into account both the frequency control channel and current channel effect.

Experimental Results:

The data of the experimental CSIM drive is given in Appendix I. It is noted that the experimental machine does not represent a typical CSIM drive. The machine's flux is programmed as follows:

I_m=0.324 pu, $0 < \tau < 0.2$,
I_m=0.682 I_r, $0.2 \leq \tau < 0.4$,
I_m=1 pu, $0.4 \leq \tau \leq 1.5$,

Where τ is the torque reference in pu.

For the experimental induction motor, it is found that linearization of torque reference to electromagnetic torque output cannot be implemented. This is because the value of the mutual inductance is large, and hence, the magnetizing current is far below the value of the torque producing component of stator current. The experimental drive has the characteristics shown in fig.12.

The time responses of the slip frequency command, link current command, link current, and rotor speed for a change in speed reference are given in fig.13. The step input of speed reference is 240 r/min, and the machine is in the steady-state at 480 r/min. The load that is presently in the machine is proportional to speed. The link current reference and slip frequency command change in time whereas the link current follows its reference in 25 ms. This is due to the fact that the value of the link filter and the stator leakage inductance are very high and amount to 128 mH. Also the voltage available to force the current in the link filter is limited to 280 v. The slow response in speed is the consequence of the large inertia of machine, its load, variable flux operation of the machine, and the limited voltage available in the dc link.The step responses for the load torque input are shown in fig.14. The steady state operating speed of the machine is 720 r/min. The magnitude of step load torque applied is 0.4 pu, over the steady-state operating torque of 0.367 pu. The drive operates in a stable condition over its entire designed speed region of 0-2400 r/min.

Speed controller requires minimum effort and is made possible due to the presence of the angle loop. Experimental results corroborate this aspect in the CSIM drive.

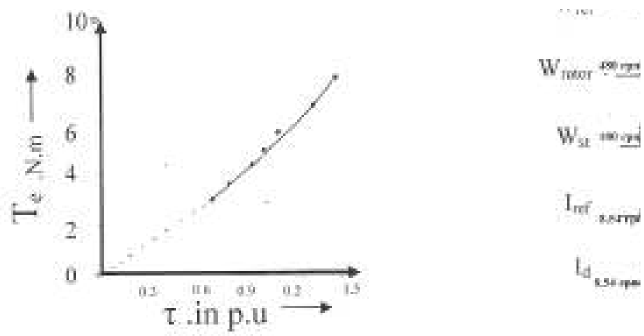

Fig. (12): Input reference to output electromagnetic torque relationship in experimental drive.

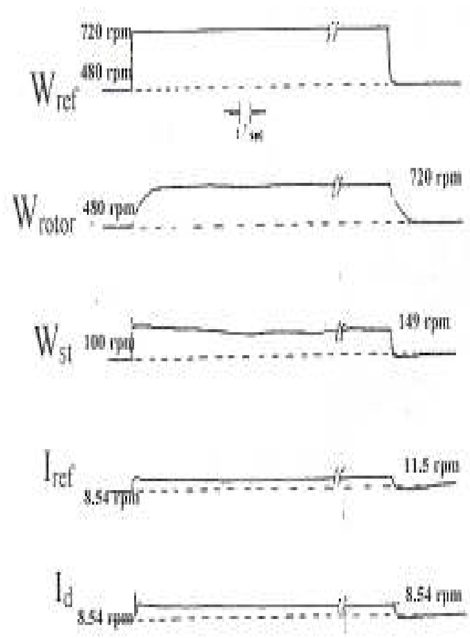

Fig. (13): Step responses for speed reference input with load proportional to speed.

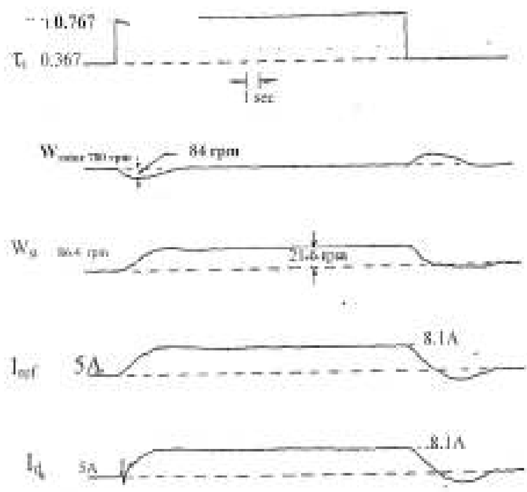

Fig. (14): Step responses for load torque input.

Conclusion:

The step-by-step design of an angle-controlled CSIM drive has been given .The physical understanding of the dynamics of the induction motor, the inverter, and its application to the design of controllers has freed designers from the need for critical design of stabilizers. Minimum turing of the stabilizing controller is needed for this scheme.

Nomenclature:

b : Delay of the front-end current source.
c : Commutation capacitance, farads.
I_d : DC link current.
I_m : Flux producing component of the stator current.
I_r :Torque producing component of the stator current.

I_{ref} : Stator current reference.
J : Moment of inertia of the induction motor and its load.
k_R : Gain of the controlled current source.
k_r : Torque constant.
L_F : DC link inductance, H.
L_m : Mutual inductance of the induction motor, H.
L_{ts} : Stator leakage inductance per phase, H.
L_{tr} : Referred rotor leakage inductance per phase, H.
P : Differential operation.
R_F : DC link resistance, Ω.
R_s : Stator resistance per phase, Ω.
S : Slip, also Laplace operator.
S_s : Slip speed, r/min.
t : Time.
T_d : Commutation delay time.
T_e : maximum Torque per Ampere
T_r : Torque producing components stator current
V_d : DC link input voltage.
V_I : Inverter input voltage.
W_e : Stator frequency, rad/s.
W_{st} : Slip frequency, rad/s.
θ : Torque angle, rad.
τ : Torque reference.

Appendix I:

Transfer functions of the controllers in the angle-controlled CSIM drive.

$$G_1(s) = \frac{k_1}{s}(1+T_1 s)\,, G_2(s) = k_2\,, G_3(s) = \frac{k_c(1+T_c s)}{s}\,, G_5(s) = k_5$$

$G_6(s)$ = transfer function of frequency compensator , $G_7(s) = k_7$

$$G_D(s) = \frac{12 - 6Td^s + Td^2 s^2}{12 + 6Td^s + Td^2 s^2}\,, G_{10}(s) = k_{10}\,, G_{11}(s) = \frac{k_{11}}{1+T_{11}^s}\,, G_{12}(s) = k_{12}\,, H_1(s) = kH_1\,,$$

$$H_2(s) = kH_2$$

Appendix II:
Experimental CSIM Drive parameters.[10]

The parameters of a 240 V, 4-hp three phase delta connected semi squirrel cage rotor are as follows:
R_s=1.85 Ω, R_r=2.128 Ω, n=1, L_{tr}=L_{ts}=9.104 mH, R_m=9569.38 Ω, J=0.1546 kg.m^2, R_f=0.4 Ω, L_f=120 mH, L_m=6379 mH, c=30 μF, k_R=56.16, k_c=10, k_1=1, k_{10}=1, k_{11}=1, k_{12}=0.004, k_{H1}=0.7235, k_{H2}=1, T_1=1, T_c=0.0312, T_{11}=0.023.

References:

1. K.P. Phillips, "*Current source converter for ac motor drives*", IEEE Trans. Ind. Appl., Vol. IA-8. pp. 679-683, Nov./Dec. 1972.
2. A.B.Plunkett,J.D.Datre,and T.A.Lipo, "*Synchronous control of a static ac induction motor drive* ",IEEE Trans. Ind. Appl., Vol. LA-15, pp. 430-437, July/August 1979.

3. L.H. Walker and P.M. Espelage, "*A high performance controlled current inverter drive*", IEEE Trans. Ind. Appl., Vol. IA-16, pp. 193-202, Mar/Apr. 1980.
4. C.E. Retting, U.S. Patent, 3962614, June, 1976.
5. R. Krishnan, W.A. Maslowski, and V.R Stevanovic, "*Control principles in current source induction motor drives*", IEEE. IAS Annu. Meeting conf. Rec., Oct. 1980, pp. 605-617. (Also accepted for publication in the IEEE. Trans. Ind. Appl.).
6. R. Krishnan, V.R. Stevanovic, and J.F. Lindsay, "*Control characteristics of inverter fed induction motor* ", IEEE-IAS Annu. Meeting conf. Rec., Oct. 1981. pp. 548-561. (Also accepted for publication in IEEE Trans. Ind.Appl.)
7. A. Joshi, "*AC traction drives using current source inverter*", Ph.D. Thesis, University of Toronto, Toronto on Canada 1982.
8. M. Showleh, W.A. Maslowski, and V.R. Stevanovic, "*An exact modeling and design of current source inverter*", Conf. Rec., IEEE-IAS Annu. Meeting, pp. 439-459, Oct. 1979.
9. L.J. Garces, "*Parameter adaptation for the speed controlled static drive with squirrel cage induction motor*", Conf. Rec., IEEE-IAS Annu. Meeting. pp. 843-850, Oct. 1979.
10. R. Krishnan,"*Control and dynamicsof inverter-fed induction motor* ", Ph.D.Thesis Concordia University, Montreal, PQ.Canada Mar. 1982.